CrossMark

ORIGINAL ARTICLE

Influence of carbon nanotubes on steel–concrete bond strength

A. Hawreen · J. A. Bogas

Abstract In this study, the bond strength between steel and concrete reinforced with multi-walled carbon nanotubes (CNTs) is analysed. To this end, pull-out tests were carried out for concretes with incorporation of 0.05–0.1% of different types of functionalized and unfunctionalized CNTs with distinct aspect ratios and dispersion techniques. The results showed that CNTs can improve both compressive strength and steel–concrete bond up to 21% and 14% respectively, as compared to plain concrete. The highest compressive strength was found in concrete with higher amounts of lower aspect ratio CNTs, while the best steel–concrete bond performance was attained for concrete with lower amounts of higher aspect ratio CNTs. CNTs were effective to retain the crack propagation, increasing the bonding stiffness and reducing the deformation of concrete consoles between steel ribs. CNTs of higher aspect ratio could better contribute with their microcrack bridging effect. Microscopic analysis confirmed the adequate dispersion and microcrack bridging provided by CNTs, delaying the macrocrack propagation within the aggregate–paste and steel–concrete interfacial transition zones.

A. Hawreen (✉) · J. A. Bogas
CERIS-ICIST, DECivil, Instituto Superior Técnico,
Universidade de Lisboa, Av. Rovisco Pais,
1049-001 Lisbon, Portugal
e-mail: hawreen.a@gmail.com

J. A. Bogas
e-mail: abogas@civil.ist.utl.pt

Abbreviations

CNTs	Carbon nanotubes
CNTCOOH	Carboxyl-functionalized nanotubes with –COOH groups and higher aspect ratio
CNTOH	Carboxyl-functionalized nanotubes with –OH groups and higher aspect ratio
CNTPL	Unfunctionalized carbon nanotubes with longer aspect ratio in the powder form
CNTSL	Unfunctionalized carbon nanotubes with longer aspect ratio in aqueous suspension
CNTSS	Unfunctionalized carbon nanotubes with shorter aspect ratio in aqueous suspension

1 Introduction

One of the approaches pursued towards the production of concrete with superior behaviour is the incorporation of nanomaterials, including carbon nanotubes (CNTs). Despite their difficulty to disperse and high cost, the incorporation of CNTs in cement based

materials has been increasingly studied [1–7] due to their outstanding mechanical properties [8, 9]. The CNTs Young's modulus can be about 6 times higher than that of steel and tensile strength was reported to be as high as about 100–150 GPa [8, 9]. Therefore, these nanomaterials, with higher aspect ratio than any other known material, have been considered ideal candidates for application in composites, being potentially able to retain the propagation of small microcracks [3, 7].

Although research on cementitious materials reinforced with CNTs is still recent, various studies have been conducted, essentially focused on the mechanical characterization of cement pastes [1, 4, 10, 11] and, in less extent, of mortars [11, 12]. One of the main obstacles to the efficient reinforcement of cement materials with CNTs is the agglomeration tendency of these nanosized materials, due to their non-polar behavior, high surface area and high aspect ratio [3], as well as the high pH environment of cementitious materials, that may destabilizes the chemical action of surfactants [3, 13]. For this reason, some studies reported the ineffective contribution of CNTs to strength improvement [12, 14]. Nevertheless, increments of compressive strength and flexural strength up to 25–35% have been reported in literature for CNTs contents up to 0.5% by weight of cement [14–16]. The positive contribution of CNTs has also been reported in increasing the flexural toughness [11, 17], as well as in reducing the water absorption, carbonation, chloride ion penetration [1, 2], shrinkage of cementitious composites [1, 11]. This improved performance of CNT-reinforced cement based materials is essentially attributed to the CNTs pore filling between the hydration products (filler effect, [18]), the availability of extra sites for the faster and more uniform growth of C–S–H (nucleation effect [1, 2]) and the enhanced stress transfer and retention of crack progression provided by CNTs crossing microcracks (bridging effect, [1, 3]). Some few studies have also been focused on the characterization of concretes reinforced with CNTs. Kerienè et al. [19] in autoclaved aerated concretes and Wille and Loh [20] in ultra-high performance concretes reported modest increments of compressive strength with the incorporation of CNTs. Carriço et al. [2] studied the mechanical and durability behaviour of concretes reinforced with 0.05–0.1% CNTs of different aspect ratios. The authors found that the incorporation of CNTs was effective to improve the mechanical strength, water absorption capillarity, carbonation and chloride penetration resistance up to 21%, 25%, 16% and 12%, respectively. The contribution of CNTs was less noticed when tests were carried out under reduced cracking conditions. Nonetheless, despite the increased research effort in this field, knowledge on CNT–concrete reinforced is still limited and further investigation is needed.

The steel–concrete bond is the phenomenon that allows the load transfer between steel reinforcement and the surrounding concrete, ensuring the composite behaviour of reinforced concrete, with great relevance in its structural behaviour. This property also affects ductility, as well as the control of deformability and cracking of reinforced concrete, limiting the width and distance between cracks [21–24]. Steel–concrete bond is ensured by adhesion, friction and mechanical mechanisms, affecting its bond stress–slip behaviour [21, 22, 25, 26]. The first phase of bond behaviour occurs by chemical adhesion, due to the physical–chemical connection between both materials. Then, pull-out of steel bars involves the generation of radial forces and cylindrical tensile stresses in concrete, especially when ribbed bars are used. As a result, transverse microcracking propagates over concrete cover and the relative displacement between concrete and steel rebar progressively increases. In this case, the concrete cover and tensile strength of concrete are major factors for enhancing the constraint effect and wedge generation [26, 27]. Depending on the confinement of concrete, debonding may occur by rebar pull-out (shear failure of steel–concrete interface) or by concrete splitting due to radial stresses. The bond-stress–slip relationship and average bonding stress may be determined by beams bending tests [28, 29] or more frequently by pull-out tests [28, 30, 31], as done in this study.

The steel–concrete bond behaviour depends on various factors, such as the direction of loading [24], the compressive and tensile strength of concrete [32], the amount of transverse reinforcement [33], the concrete composition, the concrete shrinkage, the steel properties, the concreting direction [21], the curing conditions [34], the testing procedure [22] and the steel bar anchorage length [32, 34].

The influence of steel fibers incorporation on the steel–concrete bonding has been studied by various authors [25, 27, 31, 35]. It is well-known the improved post-crack behaviour of fiber reinforced concrete, in

which fibers act as bridges to transfer stresses between cracks, controlling its opening and propagation [36]. The positive effect of steel fibers in steel–concrete bond have been shown, even at low fiber content [37]. Fibers act on reducing the crack width and increasing the passive confinement of concrete [37, 38]. Fibers also improve the toughness of bond failure [25, 39]. This is relevant on distribution of bond stresses and general improvement of steel–concrete bond behaviour. In this particular, effective fracture toughness improvement has been shown in fiber reinforced concrete [40], as well as in concrete reinforced with carbon fibers [41] and CNTs [11].

Increasing the quality of the steel–concrete interfacial transition zone (ITZ) improves the steel–concrete bond behaviour. Gjorv et al. [21] found that the incorporation of up to 16% of silica fume increased the pull-out strength, especially in high strength concrete. The presence of silica fume improved the ITZ microstructure by reducing both porosity and thickness of this zone. In addition, there is a reduction of the preferential orientation of C–H crystals and accumulation of free water at the steel-paste ITZ [21]. Elfeky et al. [42] reported that the addition of 4.5% nanosilica could increase the residual bond strength in reinforced concrete. In fact, besides their eventual reactivity, the incorporation of fine materials may contribute to the microstructure refinement of these regions by their filler and nucleation effect. On the other hand, the inclusion of fibers can improve the ITZ by reducing the crack propagation [43, 44]. In this case, the incorporation of nanofibers may simultaneously contribute by their filler, nucleation and bridging effect.

Accordingly, CNTs may act at a lower scale, contributing to the improvement of toughness, microcrack retention and quality of the ITZ. Therefore, the incorporation of CNTs potentially improves the steel–concrete bond behaviour of concrete. However, to the best of the authors' knowledge, until now, no study has been undertaken on this topic. Hence, this study aims to analyse the bond behaviour between CNT-reinforcing concrete and conventional steel reinforcement. To this end, direct pull-out tests were carried out and the influence of different types of functionalized and unfunctionalized CNTs of distinct aspect ratios was studied. Compressive strength tests and scanning electron microscopy (SEM) analysis were also

conducted to better understand the CNT reinforcement behaviour.

2 Experimental campaign

2.1 Materials

Concrete was produced with Portland cement I 42.5 R (EN 197-1 [45]) and two types of natural gravel (G) and sand (S) (Table 1): crushed limestone fine gravel, FG (0/8 mm), crushed limestone coarse gravel, CG (4/11.2 mm); fine siliceous sand (0/2 mm); coarse siliceous sand (0/4 mm).

For CNTs-reinforced concrete, five types of industrial multi-walled CNTs were selected from *Timesnano* (Table 2). CNTSL and CNTSS, with distinct aspect ratios, were supplied in aqueous suspension, at CNT concentrations of 5% and 9%, respectively. Dispersion was attained with the aid of a polyethylene glycol aromatic imidazole surfactant-TNWDIS. Pristine CNTPL had the same aspect ratio as CNTSL, but it was supplied in powder form. CNTCOOH and CNTOH, also supplied in powder form, were initially –COOH and –OH functionalized, respectively. CNTOH presented the highest aspect ratio. The anionic surfactant Dolapix PC67, based on the sodium salt of a polycarboxylic acid (–COONa), was adopted to disperse powder form supplied CNTs (CNTPL, CNTCOOH, CNTOH).

Hot-rolled steel ribbed bars of 12 mm diameter were used in the pull-out tests described in Sect. 2.4. The tensile strength of the steel bars was tested according to EN 10002-1 [46]. From four samples, the average yield strength, f_{ym}, was 413 MPa and the average ultimate strength, f_{um}, was 566 MPa.

2.2 CNTs dispersion

CNTs were previously dispersed in water before concrete mixing. This first involved the physical procedure of sonication to break CNT bundles and then the incorporation of the Dolapix PC67 surfactant to maintain the dispersion stability. The type and amount of surfactant, as well as the sonication duration were defined based on a previous study of Guedes et al. [13], using the same types of CNTs. CNTPL, CNTCOOH or CNTOH were first stirred with 40% of mixing water for a CNT to surfactant

Table 1 Physical and mechanical properties of aggregates

Property	FS	CS	FG	CG	Standard
Water absorption 24 h (%)	0.19	0.26	0.5	0.35	EN 1097-6 [72]
Oven-dried particle density (kg/m^3)	2605	2624	2646	2683	EN 1097-6 [72]
Apparent particle density (kg/m^3)	2618	2642	2698	2709	EN 1097-6 [72]
Saturated and surface-dried particle density (kg/m^3)	2610	2631	2665	2693	EN 1097-6 [72]
Loose bulk density (kg/m^3)	1569	1508	1309	1346	EN 1097-3 [73]
Voids (%)	39.76	34.74	50.53	49.82	EN 1097-3 [73]
Shape index category			SI$_{20}$	SI$_{20}$	EN 933-4 [74]
Los Angeles category			LA$_{35}$	LA$_{30}$	EN 1097-2 [75]

Table 2 Characteristics of CNTs

Notation	CNTSS	CNTSL	CNTPL	CNTCOOH	CNTOH
Commercial name	TNIM8	TNIM6	TNIM6	TNIMC6	TNIMH4
Form as supplied	Suspension	Suspension	Powder	Powder	Powder
Purity (%)	> 90	> 90	> 90	> 90	> 90
Outer diameter (nm)	> 50	20–40	20–40	20–40	10–30
Inner diameter (nm)	5–15	5–10	5–10	5–10	5–10
Length (μm)	10–20	10–30	10–30	10–30	10–30
Aspect ratio	$\sim$ 300	$\sim$ 667	$\sim$ 667	$\sim$ 667	$\sim$ 1000
True density (g/cm^3)	$\sim$ 2.1	$\sim$ 2.1	$\sim$ 2.1	$\sim$ 2.1	$\sim$ 2.1
Tap density (g/cm^3)	0.18	0.16	0.16	0.16	0.14
COOH (%)	–	–	–	1.36–1.5	–
OH (%)	–	–	–	–	2.48

mass ratio of 1:1, 1:0.5 and 1:0.25, respectively. The remaining part of the mixing water (60%) was later used to pre-saturate the aggregates (Sect. 2.3). The suspension was magnetically stirred for 4 h, followed by 30 min of sonication. CNTSS and CNTSL were already supplied in aqueous suspension, pre-stabilized with the TNWDIS surfactant. In this case, suspensions were magnetically stirred with the mixing water and sonicated for 45 and 30 min, respectively.

2.3 Mix compositions and sample preparations

Concrete mixes were produced with 380 kg/m^3 of cement (C) and w/c of 0.55 for a target slump class S3, according to EN 206-1 [47]. Although CNTs, especially acid functionalized ones, are reported to absorb water from the matrix [12] and consequently decrease the flowability of fresh concretes, the slump was found similar in both CNT-reinforced concretes and reference concrete (130 ± 20 mm). This might be related

to the small amount of well dispersed CNTs and the presence of dispersing surfactants that decreased the matrix viscosity. The ratio of C:S:G was 1:2:2.5 (by weight). The ratio for CS:FS and CG:FG were 1:1.5 and 1:2.9 (by weight), respectively. Based on a previous study concerning the mechanical behaviour of cement pastes produced with the same types of CNTs [1, 4], the optimal amount of CNTs was defined as 0.1% for CNTSS of lower aspect ratio and 0.05% for other types of CNTs with higher aspect ratios. Reference concrete (RC) without CNTs was also produced for comparison purposes. Mix compositions are indicated in Table 3.

Concretes were produced in a vertical shaft mixer with bottom discharge. The aggregates were first mixed for 3 min with 60% of the total mixing water. Then, cement and the remaining 40% of mixing water (with or without CNTs) were added and mixed for more 3 min. For each composition, three 150 mm cubic specimens were cast for compressive strength

Table 3 Mix design, compressive strength (f_{cm}), bonding stress (τ_{bm}) and maximum displacement (ΔL) of concrete mixes

Mix	Mix design			$f_{cm,28d}$			Steel–concrete bond					
	w/c	CNT type	CNT (%)	(MPa)	Δf_{cm} (%)	CV (%)	ΔL_{max}		τ_{bm}			$\tau_{bm}/f_{cm}^{1/2}$
							(mm)	CV (%)	(MPa)	$\Delta\tau_{bm}$ (%)	CV (%)	
RC	0.55	–	–	47.5	0	4.8	1.36	1.9	14.8	0	1.5	2.1
CNTPLC	0.55	CNTSS	0.1	52.1	9.6	2.3	1.04	8.2	16.9	14.1	1.8	2.3
CNTCOOHC	0.55	CNTPL	0.05	51.6	8.7	1.6	1.05	6.2	16.1	8.9	0.6	2.2
CNTSSC	0.55	CNTCOOH	0.05	57.5	21.0	4.0	1.17	2.2	16.2	9.3	1.1	2.1
CNTSLC	0.55	CNTSL	0.05	46.2	− 2.8	4.0	1.25	2.3	15.4	3.9	1.7	2.3
CNTOHC	0.55	CNTOH	0.05	50.7	6.7	2.3	1.15	4.0	15.6	5.3	1.6	2.2

and three 200 mm cubes for steel–concrete bond strength. The compaction of concrete samples was performed according to EN 12390-2 [48], using a vibrator needle with Ø25 × 160 mm and frequency of at least 120 Hz. After 24 h, samples for compressive strength test were demolded and placed in a wet chamber with relative humidity over 95% and temperature of 20 ± 2 °C until testing. Samples for pull-out tests were first placed in the wet-curing chamber for 3 days and then cured in a dry chamber with relative humidity of 50 ± 5% and temperature of 22 ± 2 °C until testing.

For pull-out tests, specimens were moulded according to Fig. 1, in which the steel bar was placed perpendicular to the casting direction, with a free length of about 50 cm at the site of load application and 2 cm at the opposite site, where the relative
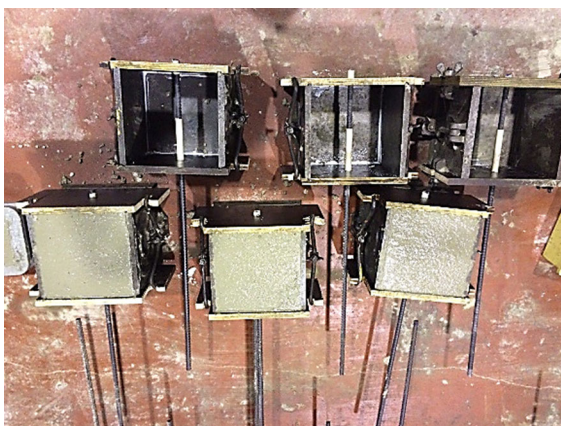
Fig. 1 Specimen production for pull-out tests

displacement was measured. The first embedded millimetres of the reinforcement were separated from the concrete by a plastic tube to set the anchoring length and to prevent stress concentration and premature concrete cone pull-out. The embedded length of the steel bar was 100 mm (about 8Ø).

For microstructural analysis, samples of about 10 × 10 × 10 mm were collected from broken specimens obtained after mechanical tests. The dispersion features of CNTs in the cement matrix were investigated by means of scanning electron microscopy (SEM) (JSM-7001F, JEOL). Before SEM analysis, samples were surface coated with a thin film of Au–Pd to ensure adequate conductivity of the electron beam.

2.4 Testing procedures

The compressive strength was determined at 28 days, according to EN 12390-3 [49]. Tests were carried out in a hydraulic press type TONI PACT 3000, for a loading rate of 0.6 MPa/s. The steel–concrete bond was characterized from pull-out tests based on RILEM 7.11.128 [50]. Tests were carried out at 28 days for a short embedment length of 8Ø. Basically, the steel bar embedded in a 200 mm cubic concrete specimen was pulled at the longer end, using a hydraulic cylinder with a tensile capacity of 112 kN and a stroke of 78 mm. This system was positioned on a load cell with a sensitivity of 1.5 mV/V and a capacity of 200 kN. The loading rate was about 0.1 kN/s, according to RILEM 7.11.128 [50]. A transducer with a stroke of 25 mm was set on the shorter unloaded end of the steel bar for measuring the relative displacement,
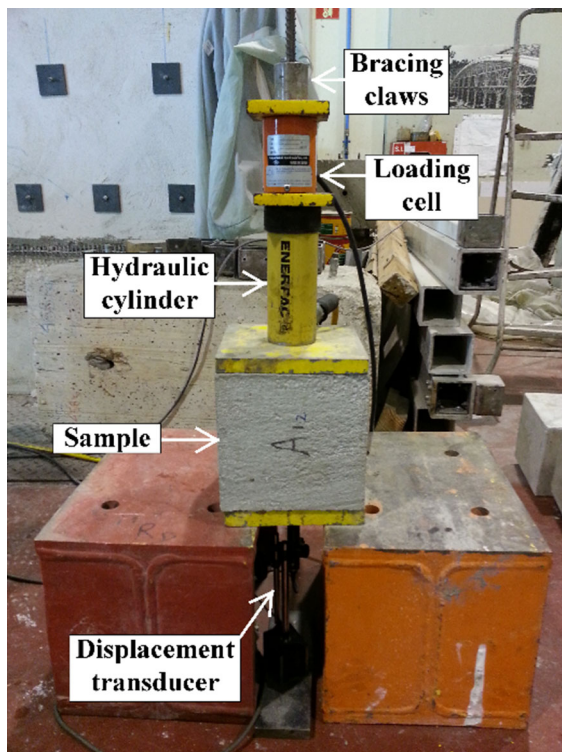
Fig. 2 Pull-out test setup

ΔL (Fig. 2). To register accurate measurements and avoid eccentricity errors during the experiment, the surface of the shorter end of the steel bar was slightly notched inward to hold the transducer's probe tip. The displacement was measured simultaneously with the load application until the steel bar was detached from the surrounding concrete.

For each concrete sample, the maximum failure load, P_{max}, and the maximum relative displacement at the maximum load, ΔL_{max}, were registered. The use of short embedment lengths ensures the nearly uniform stress distribution. In this case, the average bonding stress at the maximum load, τ_{bm} (MPa) was calculated according to Eq. (1), where P_{max} is the maximum applied force (N), l_b is the anchorage length of the steel bar (mm) and $\emptyset$ is the steel bar diameter (mm). Accordingly, the $P - \Delta L$ curves can be directly determined by measuring the pull-out force, P, as a function of the relative displacement (slip), ΔL, of the bar's free unloaded end

$$\tau_{bm} = \frac{P_{max}}{\pi \times \emptyset \times l_b}. \tag{1}$$

3 Results and discussion

The main results obtained for each composition are presented in Table 3, namely average compressive strength ($f_{cm,28d}$), relative average displacement at the free unloaded end of the reinforcement (ΔL), average bond strength (τ_{bm}) at the maximum failure load and the normalized bond strength to $f_{cm}^{1/2}$ ($\tau_{bm}/f_{cm}^{1/2}$). In the same table, the relative strength increments (Δ) compared to that of RC, and coefficients of variation (CV) between samples of the same mix are also indicated.

3.1 Compressive strength

The increment of compressive strength in CNT-reinforced concrete was as high as 21% or as low as -3%, depending on the type of CNTs. Therefore, in general, it is shown that CNTs can contribute for the strength improvement of cementitious materials. This is basically attributed to the CNTs' effect of filler [1, 2, 18], nucleation [1–3, 7] and microcrack bridging [1, 2]. The filler action leads to denser cementitious materials. The bridging effect inhibits crack growth and propagation, improves the aggregate–paste interface quality and better transfers stress between cementitious compounds [11]. The nucleation effect results from the extra sites provided by CNTs for the more homogeneous distribution and growth of hydrated products [3].

However, the mechanical strength improvement was modest. Significantly higher improvements were found in mortars [11] and especially in cement pastes [1] reinforced with the same types of CNTs. The CNTs content in concrete was limited due to their propensity to agglomerate. In addition, the presence of aggregates disturbs the uniform dispersion of CNTs, affecting the CNT spacing and their reinforcement efficiency [2, 3, 11]. Furthermore, concrete mixing is more complicated than cement paste production, which may result in poorer CNTs dispersion. Moreover, in conventional concrete, aside from the cement paste, the aggregate–paste interface also affects the mechanical strength. Therefore, the modest strength improvements may also be attributed to the CNTs' inability to significantly enhance the quality of the aggregate–paste bond. Nonetheless, the effective contribution of CNTs in retaining the microcrack propagation and densifying the cement matrix in the interface region

has been reported [11, 51]. In conclusion, the CNT-reinforcement of concrete was unattractive, at least considering the CNT dispersion method adopted in this study and the still high cost of CNTs in the market up to date. In this case, slightly decreasing the w/c of concrete can lead to similar or even higher improvement of compressive strength [2].

The type of CNTs had an important role in the compressive strength enhancement of concrete. Comparing to that of RC, the incorporation of CNTSS, CNTPL, CNTCOOH and CNTOH led to strength increments of 22%, 10%, 9%, and 7%, respectively (Table 3). The different efficiency of each CNTs type was attributed to their aspect ratio, dispersion technique and spacing within the cement matrix [2, 3, 11]. The best behaviour was found for high dosages of lower aspect ratio CNTs (CNTSS), which can be easier dispersed than the same amount of CNTs with higher aspect ratio (CNTPL, CNTCOOH, CNTOH). In fact, although CNTs with higher aspect ratio should develop higher pull-out strength in the matrix, they are more prone to agglomerate. Moreover, it was theoretically concluded that lower aspect ratio CNTSS can better ensure the force transfer in the matrix, despite the greater free spacing between them [2, 3]. In addition, experimental studies in aqueous suspensions showed that CNTSS had the lowest structural damage due to sonication and the highest dispersibility in high pH environments [13]. The reinforcement efficiency of CNTs was also strongly affected by their dispersion technique. In fact, concrete reinforced with CNTSL and CNTPL showed different performances despite containing CNTs with the same aspect ratio (Table 3). The incorporation of CNTSL had even a negative effect on the mechanical strength, leading to 3% reduction comparing to RC. This was caused by the different surfactants used to disperse the same aspect ratio CNTs (Sect. 2.2).

CNT-reinforced concrete with covalent functionalized CNTCOOH showed similar behaviour to that of concrete with untreated CNTPL of equal aspect ratio. On the other hand, concretes with the same amount of functionalized CNTOH, of higher aspect ratio (Table 1), showed slightly lower mechanical performance. This suggests that the aspect ratio assumed greater influence on the reinforcement efficiency than the functionalization of CNTs. Actually, functionalized CNTs are reported to be easily dispersed due to their greater hydrophilicity [12] and to improve the

load transfer due to the stronger chemical bond between the CNTs functional group and C–S–H phases [52]. However, the reinforcement efficiency of functionalized CNTs in cement matrix is also affected by other factors: when surfactants are used together with functionalized CNTs, as occurred in this study, the interaction between CNTs functional groups and cement matrix is affected; functionalization and sonication cause structural defects in CNTs [1, 11, 53, 54]; functionalized CNTs may demand higher water absorbance due to their hydrophilicity, which impairs the hydration process [12]; ettringite formation tends to be higher in cementitious composites reinforced with functionalized CNTs [1, 3, 53].

3.2 Steel–concrete bond strength

Contrary to what was found by Bogas et al. [26] in conventional concrete, CV of τ_{bm} was always lower than 2%, showing low test variability. Moreover, no clear difference of CV was found between CNT-reinforced and unreinforced concretes. For all tested specimens, the failure mode involved the pull-out of the reinforcement steel bar without its rupture, being possible to directly compare the bonding characteristics between different mixes. Moreover, the premature yielding of reinforcement never occurred before pull-out, which would affect the concrete-steel bonding.

In general, the $P - \Delta L$ curves were similar in CNT-reinforced concretes and RC (Fig. 3). As reported for conventional concrete with ribbed steel rods, the steel–concrete bond behaviour was characterized by the development of four main mechanisms, namely the initial chemical and micromechanical physical adhesion, friction, crushing strength of concrete near the steel ribs (wedge action) and by the interlocking effect of coarse aggregates [21, 22, 55]. In the first stage, the adhesion between the reinforcement and the concrete is activated at low stress levels and it's essentially ensured by chemical adhesion and interlocking between the mortar and the roughness of the steel surface [22]. During this phase the relative displacement between concrete and steel is minimum. In the second stage, the ribs of the steel rod are mobilized and the bond is governed by their resistance against concrete, i.e., the "wedge effect". The concentrated forces near the ribs give rise to the development of radial cracking and subsequent "consoles" are formed. During this stage the relative displacement
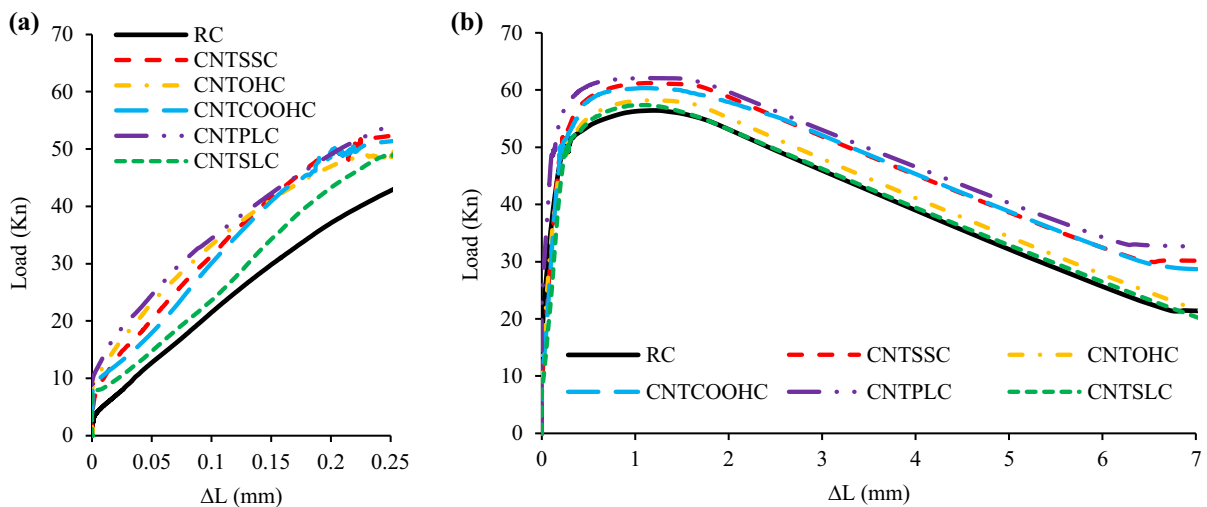
Fig. 3 Pull-out load-ΔL curves of concrete with different types of CNTs, at 28 days: **a** ΔL up to 0.25 mm; **b** global curve

of the reinforcement is related to the deformation of these consoles and the concrete crushing near the ribs [56]. The third stage is initiated after the appearance and development of the first radial cracks. According to fib10 [22], for τ_{bm} higher than about 1–3 f_{ct}, the longitudinal cracks expand radially due to the wedge effect that induces circumferential tensile stresses in concrete. In this case, the bonding strength is ensured mainly by the interlocking between the reinforcement and the concrete struts radiating from the steel rod, which are supported by the outer ring of undamaged concrete [57]. In situations of high confinement, this stage tends to be less relevant. Finally, after this stage, two failure mechanisms are possible. If the level of confinement is not enough, the radial cracking proceeds through the concrete cover and the splitting failure occurs for bond stresses lower than the maximum bond strength capacity [58]. Otherwise, the concrete consoles between ribs are sectioned, the pull-out occurs and the residual bonding strength is due to friction effects.

From Fig. 3a it was found that during the first stage of steel–concrete adhesion, the behaviour of concrete was little affected by the incorporation of CNTs. According to some authors [21, 26, 59] denser ITZ between steel and concrete may improve the chemical and physical adhesion component. In this work, except for concrete with CNTPL, this was not evident. Therefore, we may conclude that the steel–concrete adhesion was not significantly improved by the incorporation of CNTs. The addition of CNTPL

slightly improved the adhesion component, as well as the global pull-out behaviour, as discussed below (Fig. 3a).

Immediately after the first stage, when the radial cracking was developed and the concrete "consoles" were formed, it was possible to observe a progressive increase of the average bonding stress for a given relative displacement, ΔL, in concrete with CNTs. In this case, the incorporation of CNTs seems to have been effective and the bond stiffness was increased, regardless of the CNT type. This phenomenon may be attributed to the bridging effect provided by CNTs [1, 3]. In fact, CNTs may be able to retain the microcrack propagation, producing lower crack widths and hence retaining the macrocrack propagation that leads to the greater deformation of consoles and higher relative displacements. Actually, CNTs acted to delay the transition from the adhesion phase to the second phase of radial crack propagation and consoles formation. As a result, when compared to RC, concrete reinforced with CNTs showed higher bond strength (τ_{bm}) for lower relative displacements, ΔL, at the maximum failure load (Table 3). This confirms that CNTs were able to improve the bond behaviour of concrete, showing their positive action on the retention of crack-propagation.

Finally, taking into account the descending branch of the $P - \Delta L$ curves (Fig. 3b), higher residual bond strengths were obtained in CNT-reinforced concrete for a given relative displacement. This is attributed to the higher maximum bond strength attained in

concrete with CNTs, which delayed the rupture of concrete consoles between the steel ribs.

Concerning the influence of the different types of CNTs, it was found that the maximum steel–concrete bond strength improvement, when compared to RC, was registered in concrete with 0.05% CNTPL (14%), followed by those with CNTSS (9%) and CNTCOOH (9%) and then concrete with CNTOH (5%) and CNTSL (4%). Once more, the CNTSL-concrete with higher air content and poorer dispersion of CNTs showed the worst performance [1, 3].

On a global view, the greatest performance of CNTSS, CNTPL and CNTCOOH was confirmed, as found in compressive strength. As discussed in Sect. 3.1, CNTSS may better ensure the force transfer through microcracks. However, concrete with CNTSS didn't show the best performance in pull-out tests, as found for compressive strength. This suggests that powder form supplied CNTs with higher aspect ratio (CNTPL) should have been more effective in crack retention. This may be essentially attributed to the higher pull-out tensile strength and greater strain capacity of CNTs with higher aspect ratio and greater surface area to volume ratio. In other words, the bridging effect and the subsequent force transfer though microcracks showed to be more relevant in reinforced concretes with high aspect ratio CNTPL. The greater compressive strength found in concrete with CNTSS (Sect. 3.1) confirms that the dispersion was more effective and hence, the filling and nucleation effects should have been more relevant in these mixtures. However, bridging was more determinant in steel–concrete bonding than the other effects of filler and nucleation. Hawreen et al. [11] studied the mechanical characterization of mortars produced with the same CNTs types. The authors found that mortars with CNTPL attained higher fracture toughness than those with CNTSS, despite their similar compressive and flexural strength. This was also attributed to the better bridging effect provided by CNTPL. In sum, depending on the type of CNTs, the effect of filler, nucleation and bridging can be more or less relevant. In this study, CNTs of higher aspect ratio should have contributed more for the bridging effect and the well dispersed CNTSS, with lower aspect ratio, for the effects of filler and nucleation. The greatest contribution of CNTSS for the early hydration of cement paste was demonstrated elsewhere by means of thermogravimetric analysis [1].

The same behaviour was not confirmed for concrete with CNTCOOH with identical aspect ratio of CNTPL, which showed the same performance of that with CNTSS. Nevertheless, variations between different compositions were low. As for compressive strength, the worst behaviour was found in concrete with CNTSL. This shows that the dispersion procedure considered for this type of CNTs, with the same aspect ratio of CNTPL, was not adequate. Nevertheless, all studied types of CNTs were able to improve the steel–concrete bond behaviour of reinforced concretes.

In a previous investigation [60] on concrete reinforced with 3% of nanosilica, it was reported an improvement of 39% in the steel–concrete bond strength when compared to reference concrete. In this case, a much higher amount of nanosilica could be more effective than the small amount of CNTs incorporated in this study. In fact, as mentioned, the appropriate dispersion of CNTs could only be achieved at lower CNTs contents, up to 0.1%, limiting their reinforcement contribution.

Many researchers and most normative documents have suggested empirical equations for ultimate bond stress prediction [26, 61–64]. Among other parameters, such as the quality of bonding conditions and transverse reinforcement, these expressions are mainly function of the square root of concrete compressive strength and concrete cover to rebar diameter ratio. However, a poor correlation was found between the square root of compressive strength and the maximum steel–concrete bonding strength, τ_{bm}, for RC and CNT-reinforced concretes with w/c of 0.55, at 28 days (Fig. 4). This was the result of the better participation of CNTPL in steel–concrete bond behaviour, in which the bridging effect should have had a greater effect than in compressive strength, as discussed before. Nevertheless, little variation of the normalized bond strength to $f_{cm}^{1/2}$ ($\tau_{bm}/f_{cm}^{1/2}$), lower than ± 5%, was found between different concrete mixes (Table 3).

When compared to fiber-reinforced concrete, the behaviour of CNT-reinforced concrete is slightly different, because the reinforcing materials act at different scales. As mentioned in the introduction, fibers are able to transfer stress between macrocracks, controlling their opening and propagation, which improves the concrete post-cracking behaviour [25, 36–38]. However, aside from their different
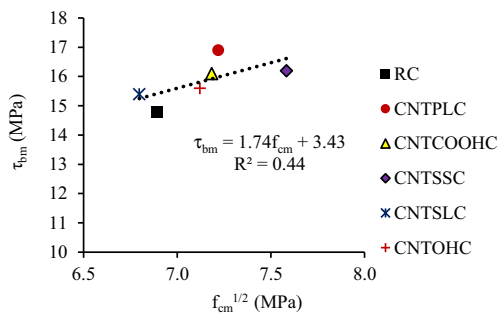
Fig. 4 Relationship between square root of compressive strength (f_{cm}) and maximum bond strength (τ_{bm}) of concretes with w/c of 0.55

chemical properties, CNTs are significantly smaller than steel fibers and can only contribute before large macro-cracks are initiated.

Due to their post-cracking behaviour, fibers are reported to improve the steel–concrete bond [25, 27]. On the one hand, they may improve the confining effect of steel bars and hence, the bond strength and bond failure ductility [27, 65, 66]. On the other hand, as steel fibers resist to crack opening caused by radial stress, the phase 2 of steel rib mobilization and wedging effect becomes more effective and the bonding strength is increased [27]. Comparing to the case of CNTs, the contribution of fibers occurs in a later stage of phase 2, after microcracks are merged into macrocracks. As shown in Fig. 3, CNTs tended to contribute in an earlier stage of steel–concrete bonding, when the radial cracks were initiated. In fact, CNTs are only able to withstand narrow microcracks of up to about 1 μm wide [3, 11].

Nevertheless, Yazici and Arel [67], considering different types and amounts of steel fibers, found only up to 16% improvement in steel–concrete bond strength. Slightly higher improvements of bond strength were attained by other authors in steel-fiber reinforced concretes. Haddad et al. [68] reported 23% increase for 2% volume of steel fibers. Similar improvements, up to 22%, were documented by Söylev [69], for concretes with 40 kg/m^3 of steel fibers. Campione et al. [57] found 7–38% higher bond strength when 0.5–2% of steel fibers, by volume, were incorporated. An improvement of 32% was obtained by Baran et al. [70] in concretes with 60 kg/m^3 of steel fibers. These improvements were not significantly higher than those obtained in the present study with low amounts of CNTs.

Beside its effect on end anchorages and lapped joints, bond affects tension stiffening and thus transverse crack width, crack spacing and curvature [22]. Due to tension stiffening, which is the ability of concrete to carry tensile stress between cracks, the stiffness of the entire element is higher than that of the single steel bar [71]. Considering the simplified load-strain relation indicated in Fig. 5 for a prismatic concrete bar loaded in axial tension, four main stages can be identified; the uncracked stage, the crack formation stage, the stabilized cracking stage and the steel yielding stage [22].

Fiber-reinforced concrete may exhibit one more stage of strain hardening behaviour, before the crack formation [22, 71]. In this stage, densely distributed cracks occur after first cracking and the slip between concrete and steel bar is still not significant [71]. Only after the peak stress of concrete has been reached the steel–concrete bond is activated and stage 3 is initiated. Moreover, contrary to plain concrete, tensile stress through the fibers can still be transmitted across the cracks, even after cracking. This ductile behaviour allows reducing the amount of tensile stress transmitted to the steel bar and thus the slip in concrete. Therefore, once the crack pattern is stabilized, two mechanisms for tensile stress transfer are mobilized, namely the concrete-steel bond and the post-cracking stress transmitted across the cracks (stage 3, Fig. 5). Basically, fibers are expected to contribute for the tension stiffening in three ways: improving the concrete peak tensile strength in the hardening stage (stage 1); improving the post-cracking behaviour of concrete (stage 3); improving the steel–concrete bond strength (stage 3).

However, as mentioned, CNTs cannot significantly contribute for the post-cracking behaviour of concrete. Considering the four stages of Fig. 5, CNTs' contribution is mainly at the third stage (stabilized cracking) when radial cracking is initiated and the concrete "consoles" are formed. In this case, the bond strength is improved and the average strain of the steel bar is reduced. CNTs can also contribute in the first stage by increasing the tensile strength of concrete, as has been reported in previous studies using the same types of CNTs [1, 11]. As a consequence, the slight contribution of CNTs to the tension stiffening leads to less spaced cracks, lower crack widths and higher flexural stiffness, thereby improving durability. The distinct effects provided by CNTs and fibers, suggests that
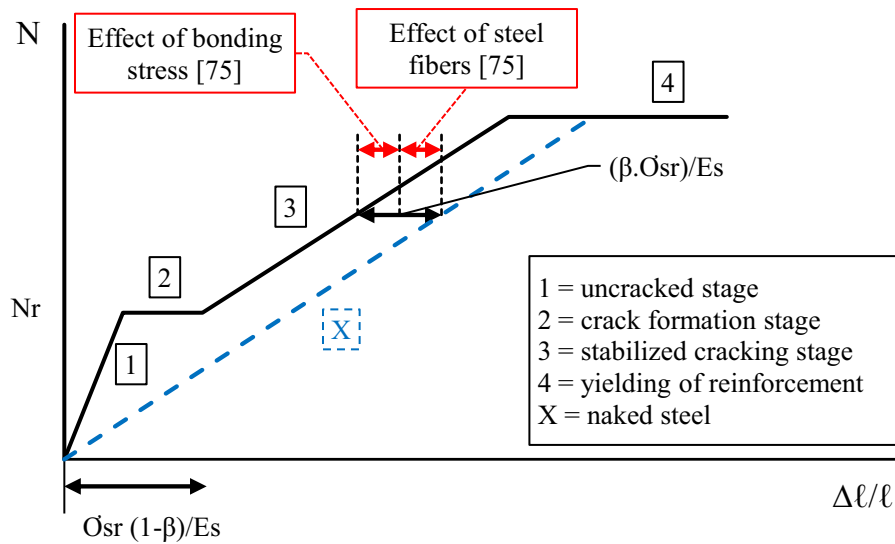
Fig. 5 Simplified load-strain relation for a centrically reinforced member subjected to tension [22]

improved solutions can be obtained with hybrid reinforcements of these materials.

3.3 SEM analysis

SEM was performed in order to confirm the participation of CNTs in concrete strengthening (Fig. 6). In general, it was possible to find regions of adequate CNTs dispersion, without significant agglomeration, where bridging was effective in microcrack retention (Fig. 6a). As found in other study concerning the mechanical strength of mortars produced with the same types of CNTs [11], nanotubes were also able to participate in retaining the microcrack propagation within the aggregate–paste ITZ region. However, no vestiges of CNTs were found at the surface of the

aggregate and in the region within about the nearest 5 μm of the surrounding matrix, regardless of the type of CNT. This suggests that the aggregate–paste bond strength was not significantly affected by the incorporation of CNTs. Nevertheless, the cement matrix in the ITZ region, which is normally up to about 40–50 μm, could have been improved, since it was confirmed the contribution of CNTs in bridging microcracks initiated from aggregates surface (Fig. 6b). The filler and nucleation effect could also contribute to the quality improvement of the ITZ [1, 3, 11]. Nevertheless, the CNTs should not be able to significantly improve the bond between the surface of the aggregate and the cement paste, having a low contribution to the mechanical strength of these regions. In fact, cracks may be developed around the
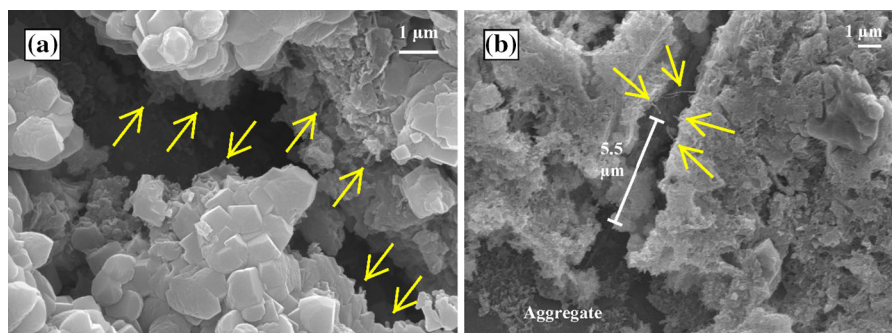

Fig. 6 SEM of concrete mixes reinforced with 0.05% CNTPL, showing, **a** CNTs uniform dispersion, **b** CNTs effect on aggregate–paste transition zone (CNTs are pointed)

surface of the aggregate without the significant participation of CNTs to bridge and retain their propagation.

Concerning the steel–concrete bond behaviour, the pull-out of steel rebar was the predominant failure mechanism (Fig. 7a), involving concrete crashing between ribs (Fig. 7b). In general, all ribs were mobilized, suggesting a nearly uniform bond stress distribution. As shown in Fig. 8b, c, CNTs were effective in bridging the microcracks propagated from the steel ribs, confirming their ability to delay the macrocrack propagation and deformation and rupture of concrete consoles. This may explain the increase of the average bonding stress for a given relative displacement found in Sect. 3.2. As a result, when compared to RC, CNT–concretes showed higher steel–concrete bond strength.

It was found that CNTs could only be effective in bridging small microcracks (Fig. 8b), bellow a critical width lower than about 1 μm, according to Hawreen et al. [3]. Increasing the applied pull-out load, developed cracks in concrete around the ribs of steel bar further broaden until the CNTs fracture (Fig. 8c). As soon as CNTs reach their ultimate tensile strength, the nanocracks propagate to macrocracks and become no longer efficient to reinforce the matrix.

Similarly to what occurs in the aggregate–paste ITZ, immediately near the steel bar surface CNTs should not significantly contribute to the steel–concrete bonding strength. In this case, the steel–concrete adhesion component is little affected by the incorporation of CNTs (Sect. 3.2), except for the quality improvement achieved on the surrounding cement matrix.

4 Conclusions

The effect of CNTs incorporation on the compressive strength and steel–concrete bond behaviour of concrete was investigated. The results draw the following conclusions:

- It was shown the potential contribution of CNTs in increasing the compressive and steel–concrete bond strength of concrete, participating in concrete reinforcement by means of their filler, nucleation and bridging effects. However, only modest improvements, up to about 20%, could be achieved.
- The compressive strength improvement of CNT-reinforced concrete was as high as 21% or as low as − 3%, compared to plain concrete. Reinforcement efficiency was affected by the type of CNTs, namely their aspect ratio, dispersion technique and nanotube spacing.
- The highest compressive strength was found in concrete with higher amounts of lower aspect ratio CNTs. Nanotubes dispersibility assumed great relevance on strengthening efficiency. Concrete with functionalized CNTs showed similar behaviour to that with pristine CNTs of equal aspect ratio.
- Regarding the steel–concrete bond behaviour, the first stage of steel–concrete adhesion was little affected by the incorporation of CNTs. However, when the radial cracking was developed CNTs were effective and the bonding stiffness was improved when compared to that of unreinforced concrete. This was attributed to the bridging effect of CNTs, which might be able to retain the crack
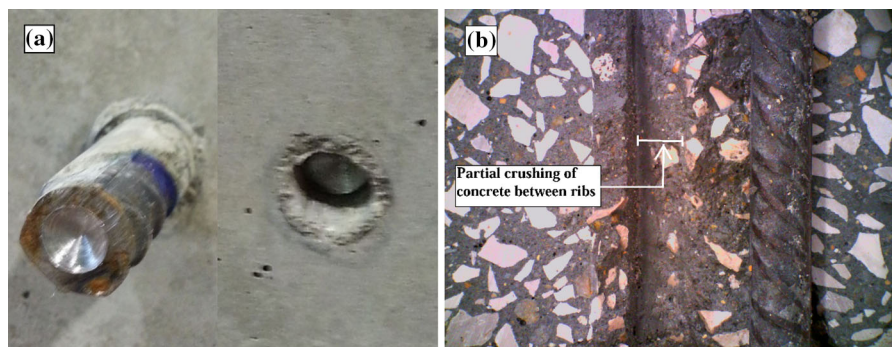

Fig. 7 Steel bar pull-out failure in concrete with 0.05% CNTPL: **a** steel bar end displacement before and after pull-out test, **b** partial crushing of concrete consoles between the steel bar ribs
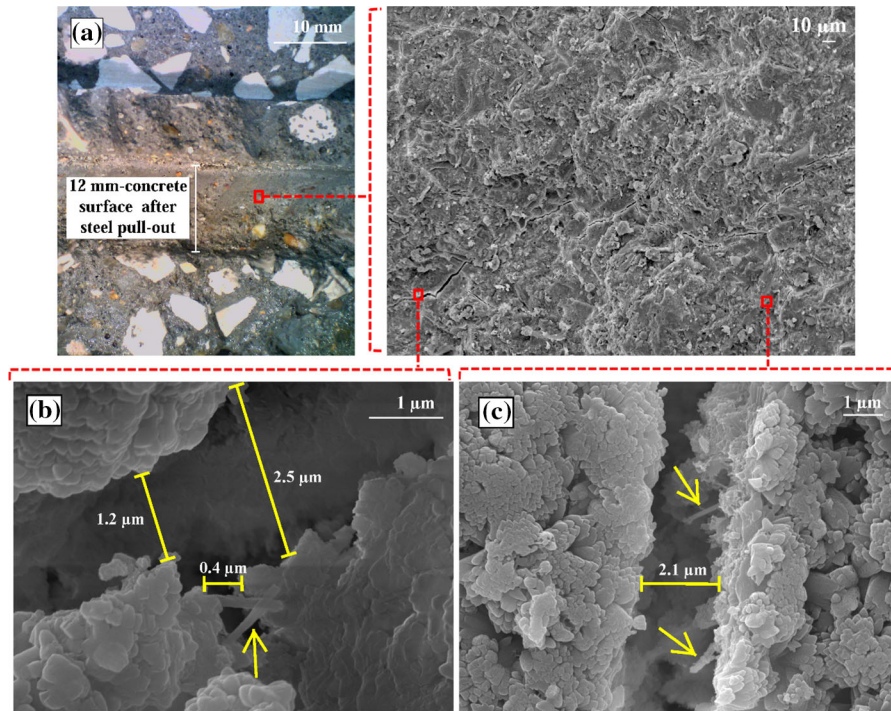
Fig. 8 **a** Images of the cement matrix immediately near the reinforcement surface. SEM showing **b** CNTs bridging, **c** CNTs rupture after pull-out tests of concrete with 0.05% CNTPL [arrows indicate CNTs (↑)]

propagation and reduce the deformation of concrete consoles between steel ribs. Higher residual bonding strength was also found in CNT-reinforced concrete for a given relative displacement due to the delayed failure of concrete consoles. It was thus demonstrated the positive contribution of CNTs to the steel–concrete bond resistance.

- The best performance, up to 14% higher bond strength than in RC, was attained in concrete with CNTs of higher aspect ratio, which were able to greatly explore the CNTs bridging effect.
- SEM analysis confirmed the adequate dispersion and efficient bridging effect of CNTs, leading to enhanced mechanical strength properties of reinforced concrete. It was shown that CNTs were effective in bridging the microcracks propagated from aggregates surface and steel bar ribs, delaying the macrocrack propagation and deformation of concrete consoles.
- In general, the modest improvement of concrete mechanical properties with the addition of CNTs was found unattractive, at least considering the CNT dispersion method adopted in this study and the still high cost of CNTs in the market up to date.

The results obtained in this study suggest that greater amounts of well-dispersed CNTs are necessary to more effectively improve the concrete performance. The relevant application of CNTs in concrete may occur after reaching the same dispersion level and reinforcement efficiency found in cement pastes and mortars. After overcoming this issue, many potential pathways of CNT application could open to enhance the properties of concrete, and as a consequence, higher demand for the material in the market can lead to a significant drop in the unreasonable cost of CNTs.

References

1. Hawreen A, Bogas J, Guedes M (2018) Mechanical behaviour and transport properties of cementitious composites reinforced with carbon nanotubes. J Mater Civ Eng 30(10):04018257. https://doi.org/10.1061/(ASCE)MT.1943-5533.0002470

2. Carriço A, Bogas JA, Hawreen A, Guedes M (2018) Durability of multi-walled carbon nanotube reinforced concrete. Constr Build Mater 164:121–133. https://doi.org/10.1016/j.conbuildmat.2017.12.221

3. Hawreen A, Bogas J, Guedes M, Pereira MFC (2018) Dispersion and reinforcement efficiency of carbon nanotubes in cementitious composites. Mag Concr Res. https://doi.org/10.1680/jmacr.17.00562

4. Hawreen A, Bogas J, Guedes M, Pereira M (9/4/2017) Mechanical characterization of cement pastes reinforced with pristine and functionalized MWCNTs. In: Materiais, XVIII Congresso da Sociedade Portuguesa de Materiais, University of Aveiro, Aveiro

5. Iijima S (1991) Helical microtubules of graphitic carbon. Nature 354:56p. https://doi.org/10.1038/354056a0

6. Dresselhaus MS, Dresselhaus G, Eklund PC (1996) Science of fullerenes and carbon nanotubes. J Am Chem Soc 118:8987

7. Makar J, Margeson J, Luh J (21/8/2005) Carbon nanotube/cement composites-early results and potential applications. In: 3rd international conference on construction materials: performance, innovation and structural implications, Vancouver

8. Yu MF, Lourie O, Dyer MJ, Moloni K, Kelly TF, Ruoff RS (2000) Strength and breaking mechanism of multiwalled carbon nanotubes under tensile load. Science 287:637–640. https://doi.org/10.1126/science.287.5453.637

9. Peng B, Locascio M, Zapol P, Li S, Mielke SL, Schatz GC, Espinosa HD (2008) Measurements of near-ultimate strength for multiwalled carbon nanotubes and irradiation-induced crosslinking improvements. Nat Nanotechnol 3:626–631. https://doi.org/10.1038/nnano.2008.211

10. Cwirzen A, Habermehl-Cwirzen K, Penttala V (2008) Surface decoration of carbon nanotubes and mechanical properties of cement/carbon nanotube composites. Adv Cem Res 20:65–73. https://doi.org/10.1680/adcr.2008.20.2.65

11. Hawreen A, Bogas JA, Dias APS (2018) On the mechanical and shrinkage behavior of cement mortars reinforced with carbon nanotubes. Constr Build Mater 168:459–470. https://doi.org/10.1016/j.conbuildmat.2018.02.146

12. Musso S, Tulliani JM, Ferro G, Tagliaferro A (2009) Influence of carbon nanotubes structure on the mechanical behavior of cement composites. Compos Sci Technol 69:1985–1990. https://doi.org/10.1016/j.compscitech.2009.05.002

13. Guedes M, Hawreen A, Bogas J, Olhero S (4/62016) Experimental procedure for evaluation of CNT dispersion in high pH media characteristic of cementitious matrixes. In: 1° congress of tests and experimentation in civil engineering, Instituto Superior Técnico, Lisbon. https://doi.org/10.5281/zenodo.164637

14. Li GY, Wang PM, Zhao X (2005) Mechanical behavior and microstructure of cement composites incorporating surface-treated multi-walled carbon nanotubes. Carbon 43:1239–1245. https://doi.org/10.1016/j.carbon.2004.12.017

15. Sobolkina A, Mechtcherine V, Khavrus V, Maier D, Mende M, Ritschel M, Leonhardt A (2012) Dispersion of carbon nanotubes and its influence on the mechanical properties of the cement matrix. Cem Concr Compos 34:1104–1113. https://doi.org/10.1016/j.cemconcomp.2012.07.008

16. Collins F, Lambert J, Duan WH (2012) The influences of admixtures on the dispersion, workability, and strength of carbon nanotube-OPC paste mixtures. Cem Concr Compos 34:201–207. https://doi.org/10.1016/j.cemconcomp.2011.09.013

17. Zou B, Chen SJ, Korayem AH, Collins F, Wang CM, Duan WH (2015) Effect of ultrasonication energy on engineering properties of carbon nanotube reinforced cement pastes. Carbon 85:212–220. https://doi.org/10.1016/j.carbon.2014.12.094

18. Nochaiya T, Chaipanich A (2011) Behavior of multi-walled carbon nanotubes on the porosity and microstructure of cement-based materials. Appl Surf Sci 257:1941–1945. https://doi.org/10.1016/j.apsusc.2010.09.030

19. Kerienè J, Kligys M, Laukaitis A, Yakovlev G, Špokauskas A, Aleknevičius M (2013) The influence of multi-walled carbon nanotubes additive on properties of nonautoclaved and autoclaved aerated concretes. Constr Build Mater 49:527–535. https://doi.org/10.1016/j.conbuildmat.2013.08.044

20. Wille K, Loh K (2010) Nanoengineering ultra-high-performance concrete with multiwalled carbon nanotubes. Res Rec, Transp. https://doi.org/10.3141/2142-18

21. Gjorv OE, Monteiro PJM, Mehta PK (1990) Effect of condensed silica fume on the steel–concrete bond. ACI Mater J 87:573–580. https://www.concrete.org/publications/acimaterialsjournal.aspx%22

22. fib10 (2000) Bond of reinforcement in concrete. Bulletin 10, State-of-art-report. Lausanne: fib—CEB-FIP—Fédération internationale du béton

23. Walraven J, Stroband J (1995) Bond, tension stiffening and crack width control in lightweight concrete. In: International symposium on structural lightweight aggregate concrete, Sandefjord

24. Bogas J (2011) Characterization of structural concrete with light aggregates of expanded clay. Dissertation, Instituto Superior Técnico (**in Portuguese**)

25. Garcia-Taengua E, Martí-Vargas JR, Serna P (2016) Bond of reinforcing bars to steel fiber reinforced concrete. Constr Build Mater 105:275–284. https://doi.org/10.1016/j.conbuildmat.2015.12.044

26. Bogas J, Gomes M, Real S (2014) Bonding of steel reinforcement in structural expanded clay lightweight aggregate concrete: the influence of failure mechanism and concrete composition. Constr Build Mater 65:350–359. https://doi.org/10.1016/j.conbuildmat.2014.04.122

27. Bae BI, Choi HK, Choi CS (2016) Bond stress between conventional reinforcement and steel fibre reinforced reactive powder concrete. Constr Build Mater 112:825–835. https://doi.org/10.1016/j.conbuildmat.2016.02.118

28. Filho FM, El Debs MK, El Debs HC (2008) Bond-slip behavior of self-compacting concrete and vibrated concrete using pull-out and beam tests. Mater Struct 41:1073–1089. https://doi.org/10.1617/s11527-007-9307-0

29. Larrard F, Schaller I, Fuchs J (1993) Effect of the bar diameter on the bond strength of passive reinforcement in high-performance concrete. ACI Mater J 90:333–339. Retrieved from https://www.concrete.org/publications/internationalconcreteabstractsportal.aspx?m=details&ID=3888

30. Rostásy FS, Hartwich K (1988) Bond deformed reinforcing bar embedded in steel fibre reinforced concrete. Int J Cem Compos Lightweight Concr 10:151–158. https://doi.org/10.1016/0262-5075(88)90003-6

31. Dancygier AN, Katz A, Wexler U (2010) Bond between deformed reinforcement and normal and high-strength concrete with and without fibers. Mater Struct 43:839–856. https://doi.org/10.1617/s11527-009-9551-6

32. Lorrain M, Khelafi H (1988) On the resistance of high strength steel-concrete bond. Ann l'ITBTP 470:117–128 (**in French**). Retrieved from http://worldcat.org/issn/00202568

33. Neville A (1995) Properties of concrete. Pitman Publishing Comp. Ltd., New York

34. Almeida I (1990) High strength and durability concrete. Composition and characteristics. Dissertation, Laboratório Nacional de Engenharia Civil (**in Portuguese**)

35. Harajli M, Hamad B, Karam K (2002) Bond-slip response of reinforcing bars embedded in plain and fiber concrete. J Mater Civ Eng 14:503–511. Retrieved from https://www.concrete.org/publications/internationalconcreteabstractsportal/m/details/id/502

36. Bentur A, Mindess S (1990) Fibre reinforced cementitious composites. Elsevier Applied Science, London

37. Esfahani R, Rangan V (1998) Local bond strength of reinforcing bars in normal strength and high-strength concrete (HSC). ACI Struct J 95:96–106. Retrieved from https://www.concrete.org/publications/internationalconcreteabstractsportal/m/details/id/530

38. Orangun CO, Jirsa JO, Breen JE (1977) A reevaluation of test data on development length and splices. ACI Struct J 74:114–122. Retrieved from https://www.concrete.org/publications/internationalconcreteabstractsportal/m/details/id/530

39. Park R, Paulay T (1975) Reinforced concrete structures. Wiley, London

40. Banthia N, Sappakittipakorn M (2007) Toughness enhancement in steel fiber reinforced concrete through fiber hybridization. Cem Concr Res 37:1366–1372. https://doi.org/10.1016/j.cemconres.2007.05.005

41. Chen P, Chung DDL (1993) Concrete reinforced with up to 0.2 vol% short carbon fibres. Composites 24:33–52. https://doi.org/10.1016/0010-4361(93)90261-6

42. Elfeky M, Serag M, Yasien A, Elkady H (2016) Bond strength of nano silica concrete subjected to corrosive environments. ARPN-JEAS 11:13909–13924. Retrieved from http://www.arpnjournals.com/jeas/

43. Zacharda V, Němeček J, Štemberk P (2017) Micromechanical performance of interfacial transition zone in fiber-reinforced cement matrix. IOP Conf Ser Mater Sci Eng. https://doi.org/10.1088/1757-899x/246/1/012018

44. Park SH, Kim DJ, Ryu GS, Koh KT (2012) Tensile behavior of ultra high performance hybrid fiber reinforced concrete. Cem Concr Compos 34:172–184. https://doi.org/10.1016/j.cemconcomp.2011.09.009

45. EN197-1 (2011) Cement. Composition, specifications and conformity criteria for common cements

46. EN10002-1 (2001) Tensile testing of metallic materials. Method of test at ambient temperature

47. EN206-1 (2000) Concrete. Specification, performance, production and conformity

48. EN12390-2 (2009) Testing hardened concrete. Making and curing specimens for strength tests

49. EN12390-3 (2009) Testing hardened concrete. Compressive strength of test specimens

50. RILEM7.11.128 (1970) Essais portant sur ládhérance des armatures du béton. 2-Essais par traction. Bond test for reinforcing steel. Matériaux et constructions 3:175–178

51. Song X, Shang S, Chen D, Gu X (2017) Multi-walled carbon nanotube reinforced mortar-aggregate interfacial properties. Constr Build Mater 133:57–64. https://doi.org/10.1016/j.conbuildmat.2016.12.034

52. Li Y, Wang M, Zhao X (2007) Pressure-sensitive properties and microstructure of carbon nanotube reinforced cement composites. Cem Concr Compos 29:377–382. https://doi.org/10.1016/j.cemconcomp.2006.12.011

53. Abu Al-Rub RK, Ashour AI, Tyson BM (2012) On the aspect ratio effect of multi-walled carbon nanotube reinforcements on the mechanical properties of cementitious nanocomposites. Constr Build Mater 35:647–655. https://doi.org/10.1016/j.conbuildmat.2012.04.086

54. Chen SJ, Collins FG, Macleod AJN, Pan Z, Duan WH, Wang CM (2011) Carbon nanotube–cement composites: a retrospect. IES J Part A Civ Struct Eng 4:254–265. https://doi.org/10.1080/19373260.2011.615474

55. Haskett M, Oehlers DJ, Mohamed MS (2008) Local and global bond characteristics of steel reinforcing bars. Eng Struct 30:376–383. https://doi.org/10.1016/j.engstruct.2007.04.007

56. Lutz A, Gergely P (1967) Mechanisms of bond and slip of deformed bars in concrete. ACI J Proc 62-64:711–721

57. Campione G, Cucchiara C, Mendola L, Papia M (2005) Steel–concrete bond in lightweight fiber reinforced concrete under monotonic and cyclic actions. Eng Struct 27:881–890. https://doi.org/10.1016/j.engstruct.2005.01.010

58. Abrishami H, Mitchell D (1992) Simulation of uniform bond stress. ACI Mater J 89:161–168. https://www.concrete.org/publications/internationalconcreteabstractsportal/m/details/id/2237

59. Sonebi M, Davidson R, Cleland D (2011) Bond between reinforcement and concrete—influence of steel corrosion. In: 12th international conference on durability of buildings materials and components, Porto

60. Serag M, Yasien A, Elfeky M, Elkady H (2017) Effect of nano silica on concrete bond strength modes of failure. Int J Geom 12(29):73–80

61. ACI318-11 (2011) Building code requirements for structural concrete

62. CSA (1994) Design of concrete structures for buildings. CAN3-A23.3-94

63. NZS3101 (2006) New Zealand concrete structures standards
64. Eligehausen R, Popov EG, Bertero VV (1983) Local bond stress–slip relationships of deformed bars under generalized excitations, Berkeley
65. Cairns J, Plizzari GA (2004) Bond behaviour of conventional reinforcement in fibre reinforced concrete, Varenna
66. García-Taengua E, Arango S, Martí-Vargas JR, Serna P (2014) Flexural creep of steel fiber reinforced concrete in the cracked state. Constr Build Mater 65:321–329. https://doi.org/10.1016/j.conbuildmat.2014.04.139
67. Yazıcı S, Arel HS (2013) The effect of steel fiber on the bond between concrete and deformed steel bar in SFRCs. Constr Build Matter 40:299–305
68. Haddad RH, Al-Saleh RJ, Al-Akhras NM (2008) Effect of elevated temperature on bond between steel reinforcement and fiber reinforced concrete. Fire Saf J 5:334–343
69. Söylev TA (2011) The effect of fibers on the variation of bond between steel reinforcement and concrete with casting position. Constr Build Mater 25(4):1736–1746
70. Baran E, Akis T, Yesilmen S (2012) Pull-out behavior of prestressing strands in steel fiber reinforced concrete. Constr Build Mater 28(1):362–371
71. Yang Y, Walraven JC, den Uijl JA (2009) Combined effect of fibers and steel rebars in high performance concrete. HERON 54(2–3):205–224
72. EN1097-6 (2013) Tests for mechanical and physical properties of aggregates. Determination of particle density and water absorption
73. EN1097-3 (1998) Tests for mechanical and physical properties of aggregates. Determination of loose bulk density and voids
74. EN933-4 (2008) Tests for geometrical properties of aggregates. Determination of particle shape. Shape index
75. EN1097-2 (2010) Tests for mechanical and physical properties of aggregates. Methods for the determination of resistance to fragmentation